$\delta^{13}C$ signatures of organic aerosols: Measurement method evaluation and application in a source study

Katrin Zenker [a], Carmina Sirignano [b], Angelo Riccio [c], Elena Chianese [c], Carlo Calfapietra [d], Maria Vittoria Prati [e], Agne Masalaite [f], Vidmantas Remeikis [f], Emily Mook [a], Harro A.J. Meijer [a], Ulrike Dusek [a,*]

[a] *Centre for Isotope Research (CIO), Energy and Sustainability Institute Groningen (ESRIG), University of Groningen, 9747 AG, Groningen, the Netherlands*
[b] *Centre for Isotope Research on Cultural and Environmental Heritage (CIRCE), Department of Mathematics and Physics, University of Campania "Luigi Vanvitelli", 81100, Caserta, Italy*
[c] *Department of Science and Technology, Parthenope University of Naples, 80143, Napoli, Italy*
[d] *Institute of Research on Terrestrial Ecosystems (IRET), National Research Council (CNR), 05010, Porano, Italy*
[e] *Istituto Motori CNR, 80125, Napoli, Italy*
[f] *Department of Nuclear Research, State Research Institute, Center for Physical Sciences and Technology, LT-02300, Vilnius, Lithuania*

A R T I C L E   I N F O

A B S T R A C T

Analysis of the stable carbon isotope ^{13}C in organic carbon (OC) can give insight into sources and atmospheric processing of carbonaceous aerosols, provided the ^{13}C source signatures are known. However, only few data on ^{13}C signatures of OC emitted by common sources of carbonaceous aerosol are available in Europe. We present and evaluate an improved version of a measurement method to obtain $\delta^{13}C$ signatures on organic aerosols desorbed from filter samples at three different desorption temperatures (200 °C, 350 °C and 650 °C) and apply it in a source study.

With our calibration approach, the reproducibility of a L-Valine reference material desorbed at a single temperature step of 650 °C shows a standard deviation of 0.19‰ over a period of more than one year. The average $\delta^{13}C$ value for this reference material over 248 measurements is −24.10‰, which shows only a slight bias to the nominal value of −24.03‰. Repeated analysis of ambient filter samples desorbed at three temperature steps show typical standard deviations of about 0.3‰ for all temperature steps (200 °C, 350 °C and 650 °C). Isotopic fractionation due to partial thermal desorption during the individual temperature steps was tested on single compound reference materials. It showed significant isotopic fractionation only at temperature steps, in which a very minor fraction of the compound was desorbed. Possible isotope effects caused by charring of organic material were investigated and found to be not significant.

The thermal desorption method was applied to various source filter samples from the region of Naples, Italy. We analyzed two different biomass burning sources, exhaust from a city bus and traffic emissions collected in a tunnel and compared these to ambient filter samples from the same region. $\delta^{13}C$ signatures of the total OC show values in a narrow range of about −28‰ to −26‰ for all sources, which does not allow a source apportionment only based on ^{13}C. Nevertheless, the results add information to a source inventory of $\delta^{13}C$, where information of ^{13}C in organic aerosol from specific emission sources are rare. City bus emissions show little variation of $\delta^{13}C$ over the temperature steps, whereas biomass burning aerosol is enriched in ^{13}C for OC desorbed at 650 °C.

* Corresponding author.
  E-mail address: u.dusek@rug.nl (U. Dusek).

For PM10 samples in the urban tunnel an enrichment in δ^{13}C at the 650 °C temperature steps was observed, which is likely caused by the contribution of carbonate carbon to the carbonaceous material desorbed at this temperature step.

1. Introduction

Research on airborne fine particulate matter (PM) is of crucial interest as PM can have a significant influence on human health [e.g. (Nel, 2005; Pope III & Dockery, 2006)] and plays an important, but not yet completely understood and quantified, role in climate change [e.g. (Boucher et al., 2013; Myhre et al., 2013)]. Carbonaceous constituents form a major part of the PM mass concentration (Pöschl, 2005). Better knowledge about origins and properties of carbonaceous aerosol will improve global climate models and help to optimize regional air pollution control strategies.

Carbon in aerosol particles can be operationally divided into organic carbon (OC) and elemental carbon (EC), which add up to total carbon (TC). Scientific research into carbonaceous aerosols in the past years, has used chemical, optical or isotopic methods, where the most investigated isotope is the rare stable isotope ^{13}C. The majority of the isotope studies [e.g. (Aguilera & Whigham, 2018, Martinelli, Camargo, Lara, Victoria, & Artaxo, 2002, Widory et al., 2004, Narukawa, Kawamura, Li, & Bottenheim, 2008, Masalaite et al., 2015, Agnihotri et al., 2011)], investigate the stable carbon ^{13}C isotopic composition of TC collected on filter samples from ambient air. This information is often used for source apportionment studies and can be an essential input parameter to identify specific sources, especially in regions where sources show clearly different ^{13}C signatures [e.g. (Masalaite, Holzinger, Remeikis, Röckmann, & Dusek, 2017, Ni et al., 2018, Martinelli et al., 2002)]. For example carbon from C3 and C4 plants shows distinctively different ^{13}C signatures (O'Leary, 1988) of −22‰ to −33‰, and −10‰ to −18‰ respectively, because of the different biochemical pathways of carbon fixation during photosynthesis of these plants. Furthermore, it was shown that it is possible to distinguish marine from continental sources at remote coastal or marine sites [e.g. (Chesselet, Fontugne, Buat-Ménard, Ezat, & Lambert, 1981, Cachier, Buat-Ménard, Fontugne, & Chesselet, 1986, Ceburnis et al., 2011)]. In specific regions, the commonly used fossil fuel type shows a clearly different ^{13}C signature from other sources, such as e.g. biomass burning, because of the origin of the crude oil from which the fuel was produced (Garbaras et al., 2015; Mašalaitė, Garbaras, & Remeikis, 2012).

Often the ^{13}C signature found in the ambient aerosol is implicitly assumed to be identical to the ^{13}C signature of the raw source material, e.g. fossil fuel, wood or other plant material. However, it has been shown that isotopic fractionation is associated with the formation of aerosol particles [e.g. (Garbaras et al., 2015, Widory, 2006)]. A comprehensive inventory of ^{13}C signatures of aerosol produced from possible source materials can help to improve source studies of ambient aerosol using ^{13}C.

The ^{13}C signature of EC of ambient aerosol closely reflects the signature of the source as elemental carbon is generally assumed to be chemically inert and once formed its ^{13}C signature does not change significantly anymore. On the other hand, the carbon isotopic signature of the organic fraction of the aerosol can change due to atmospheric transformation processes, such as photochemical processing [e.g. (Kirillova et al., 2013, Gensch, Kiendler-Scharr, & Rudolph, 2014, Huang et al., 2006, Martinsson et al., 2017)]. Separate measurement of the stable carbon isotopic signature in EC and OC instead of the bulk TC allows a more precise apportionment of the sources and gives the possibility to investigate transformation processes of the aerosol in the atmosphere. Only a few studies [e.g. (Huang et al., 2006, Ho et al., 2006, Cao et al., 2011)] so far provide results for the ^{13}C signature in EC and OC separately. Oxidative processing of primary emitted aerosol gradually produces more refractory organic aerosol (Donahue, Robinson, & Pandis, 2009; Masalaite et al., 2017). As different refractiveness is associated with different processing time of the aerosol, a further division of the OC according to desorption temperature allows potentially a more detailed characterization of atmospheric transformation processes [(Ni et al., 2019), and references therein].

In this work we present and evaluate a measurement method to determine the ^{13}C signature in OC at three different desorption temperatures (200 °C, 350 °C and 650 °C), which is a further development of the method described in (Dusek et al., 2013). Additionally the method is applied to determine the stable isotopic carbon signature of OC emitted by sources such as biomass burning or fossil fuel
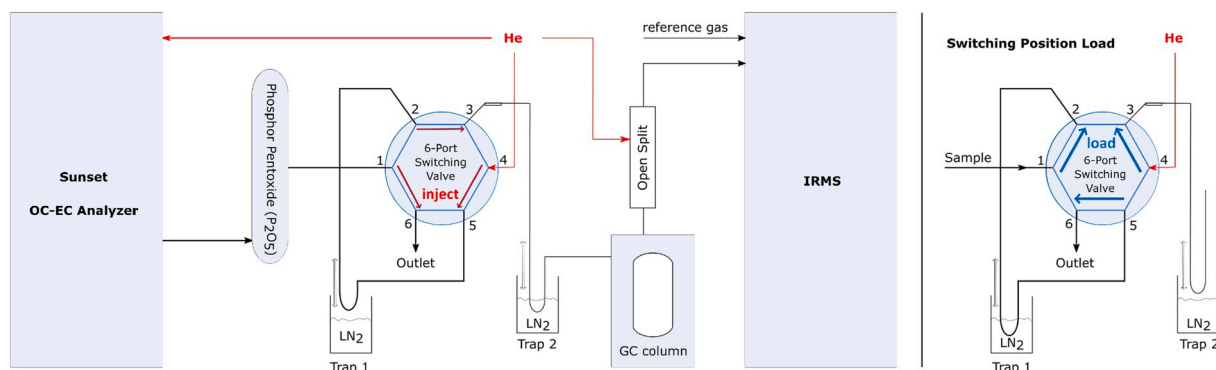

Fig. 1. Setup to measure δ^{13}C signatures (for further explanation see section 2.1.1).

combustion and ambient OC to expand the limited inventory of ^{13}C source signatures.

2. Methods

2.1. Measurement of $\delta^{13}C$ signatures

2.1.1. System setup

The system used to measure δ^{13}C signatures consists of the OC-EC analyzer (Sunset Laboratory Inc., Model 5L, see 2.2) and a continuous flow isotope ratio mass spectrometer (IRMS) model 'Optima' from 'Micromass' (now 'Isoprime'). Both instruments are connected via a custom-made interface to collect, purify and focus CO_2 extracted from the aerosol sample. The system setup is similar to the one described in (Dusek et al., 2013) and an overview is shown in Fig. 1. This setup is made and optimized to analyze δ^{13}C in organic carbon released from aerosol filter samples heated at different temperature steps in a helium carrier gas. The filter sample is placed in the front-oven of the Sunset OC-EC analyzer, where the temperature is changed according to custom made protocols. The full oxidation of all desorption products is guaranteed by the manganese dioxide (MnO_2) catalyst in the back-oven of the Sunset OC-EC analyzer. The oxidized desorption products exit the Sunset OC-EC analyzer under a constant stream of helium and are flushed through a water-trap filled with hygroscopic phosphorus pentoxide (P_2O_5). Next the sample reaches a six-port-valve, which can switch between two different positions. During the desorption process the six-port-valve is in the 'load' position (see Fig. 1) and the desorption products are flushed through trap 1, which is submerged in liquid nitrogen. All desorption products, at this point mainly CO_2, but also likely NO_x and SO_2, with sufficiently low vapor pressure are collected in trap 1. The rest of the gases exit the system through the vent. When the collection is completed, the six-port-valve is switched to the 'inject' position. Now the gas flow from the Sunset OC-EC analyzer is directly vented to the lab. Trap 1 is now thawed and brought to room temperature, and flushed with a separate helium stream from the opposite direction. The sample is purged from trap 1 to the focus trap 2 where it is collected again in liquid nitrogen. Later the liquid nitrogen is lowered from trap 2 and the sample enters a gas chromatography (GC) column, where the CO_2 is separated from the remaining gases. Then the pure CO_2 passes a custom-made open split inlet and from there it enters the IRMS. A reference gas is added separately to the helium flow shortly before entering the IRMS.

2.1.2. Measurement procedure

The whole setup, mainly the lifting and lowering of the traps, the switching of the six-port-valve and the IRMS, is controlled by a programmable logic controller (PLC). The temperature and gases in the Sunset OC-EC analyzer are controlled with a custom defined temperature protocol. It starts with a 40 s purging step with helium at room temperature to flush the system. Then the temperature is set to the requested value for a duration of 5 min 30 s and within this time the set temperature is reached after approximately 100 s. During the desorption of the sample in the Sunset OC-EC analyzer the six-port-valve is in the 'load' position and the dewar with liquid nitrogen is lifted at trap 1. 240 s after the beginning of the temperature step, the liquid nitrogen is lowered from trap 1 and the six-port-valve is switched into the 'inject' position. This means that the filter sample is at the target temperature while trap 1 is active for approximately 140 s, which is sufficient time for the desorption of average filter samples. The six-port-valve remains in the 'inject' position for 60 s to transfer the sample gases from trap 1 to trap 2. Then the six-port-valve is switched back to the 'load' position and the temperature in the Sunset oven is raised to the next target temperature, to start the collection of desorption products from the next temperature step. When all temperature steps of the measurement are completed, the analysis is finished with a cleaning step. The oven is purged for 4 min with a mixture of helium and 2% oxygen and the temperature is increased to 850 °C. This leads to a complete removal of all remaining carbon from the filter sample and avoids a carry-over of contamination to the next measurement.

Aerosol filters are normally analyzed with a protocol of three temperature steps of 200 °C, 350 °C and 650 °C. The temperature protocol to analyze reference materials consists of only one temperature step of 650 °C in helium.

A series of reference materials is measured at the beginning and the end of each measurement day. The reference materials are 'CAF' and 'CAN', which are in-house reference materials measured regularly at CIO, and 'LVal', which is an internationally agreed upon secondary reference material (Schimmelmann et al., 2016). 'CAF' and 'CAN' are both caffeines with 'CAN' enriched in ^{13}C. Their respective nominal δ^{13}C values determined at CIO are −38.2‰ and 0.61‰ (w.r.t. VPDB, see 2.1.3) with an uncertainty below 0.15‰. 'LVal' is an amino acid and its reference value δ^{13}C is −24.03 ± 0.04‰. A specific amount (5 µl for normal routine use) of an aqueous reference material solution is applied to a clean piece of quartz filter, which is then dried in the Sunset OC-EC analyzer for 2 min at 110 °C before analysis.

2.1.3. $\delta^{13}C$ calculation

The ^{13}C content of a sample is expressed in the delta notation as δ^{13}C, which is defined as follows:

$$\delta^{13}C = \frac{\left(\frac{^{13}C}{^{12}C}\right)_{sample}}{\left(\frac{^{13}C}{^{12}C}\right)_{reference}} - 1 \tag{1}$$

These delta values are usually expressed in ‰, and are reported on the international Vienna Pee Dee Belemnite (VPDB) scale. A ^{17}O correction is applied according to (Allison, Francey, & Meijer, 1995; Craig, 1957). When measuring isotopic ratios on an IRMS, a scale contraction often occurs, which can change over time. This is calibrated by measuring known reference materials and applying a

two-point linear scale correction, in our case using the reference materials 'CAF' and 'CAN'. Furthermore the two-point linear scale correction is applied to a third reference material ('LVal'), whose $\delta^{13}C$ value is close to expected values from samples, and serves as quality control. On a daily basis the mentioned reference materials cover only a very narrow OC mass range of 13 µg to 18 µg, which means that all corrections are optimized for this mass range. Real aerosol particle filter samples cover a much wider OC mass range especially because they are analyzed at different temperature steps. Considering this, a mass dependency test was performed regularly with varying amounts of 'LVal', corresponding to OC masses in the range of approximately 3 µg to 30 µg. For two time periods during which measurements for this work have been taken, a mass dependency was observed. Results for samples measured in this time periods have been corrected according to the linear relation of OC mass and the $\delta^{13}C$ values shown in the appendix (see Fig. A.1). Mass dependencies are quite common for continuous flow IRMS, and are usually thought to be caused by non-linear responses of the signal amplifiers, combined with slight deviations of the (electronic) zero. Such a dependency usually varies over time, for example by slight changes in the tuning of the IRMS.

2.2. Measurement of OC-EC concentrations

OC-EC concentrations were measured with the commercial thermo-optical OC-EC analyzer (Model 5L) from 'Sunset Laboratory Inc.' using the EUSAAR_2 protocol (Cavalli, Viana, Yttri, Genberg, & Putaud, 2010). The measured OC-EC concentrations are corrected for the instrument blank. Measurement uncertainties are automatically calculated by the instrument software and are comprised of a fixed value for the detection limit and a relative portion accounting for the random variations in the measurement.

The filter samples from the combustion of 'Quercus ilex' oak wood were treated with an additional water extraction step, as they contained high TC concentrations in the range of 73 µg/cm² to 150 µg/cm². As reported and discussed in (Piazzalunga, Bernardoni, Fermo, Valli, & Vecchi, 2011; Subramanian, Khlystov, & Robinson, 2006; Zenker et al., 2017) very high filter loading can cause an underestimation of EC on untreated filters. Water-extraction mitigates this problem and results in a more reliable EC concentration measurement. For this reason, filter samples 'Quercus ilex' have been water-extracted and the reported OC/EC ratios for these samples are calculated with OC measured on untreated filter and EC measured on water-extracted filter.

2.3. Sampling

2.3.1. Biomass burning

Experiments for the sampling of particulate matter from biomass burning were conducted at the Institute of Research on Terrestrial Ecosystems (IRET) and National Research Council (CNR) in Porano, Italy. Controlled combustion took place in a combustion chamber, described in (Lusini, Pallozzi, Corona, Ciccioli, & Calfapietra, 2014), with extraction of the particulate matter from the center of the exhaust chimney via an isokinetic sampling line onto quartz fiber filters. Two types of biomass were burned: small twigs of Quercus ilex, which is an evergreen oak common in the Mediterranean region and a commercial type of pellets made from fir wood.

2.3.2. Urban tunnel

Sampling in the urban tunnel was done similar to the experiments described in (Riccio et al., 2016, 2017), where more detailed information about the sampling location can be found. Briefly a 'Skypost PM HV model' automated sampling system by 'Tecora' with a PM10 sampling head and a volume flow rate of 2.3 m³/h was placed in the middle of a tunnel. The '4 Giornate' tunnel is part of a main city traffic street, which connects two densely populated districts in the urban area of Naples. It gives a good average over the total urban vehicle fleet ranging from mopeds, passenger cars to heavy-duty vehicles and buses. In the time period from the 28th of February 2017 to the 2nd of March 2017 six filter samples have been collected with varying sampling duration ranging from 2 h 18 min to 5 h 6 min.

2.3.3. Bus exhaust

The particulate matter from bus exhaust was sampled by installing the vehicle on a chassis dyno bench. The bus, complying with Euro III emission standard and without after-treatment systems, was driven during an urban drive cycle representative of its normal use; the experimental activity was carried out under the supervision of CNR - Istituto Motori (IM) in July 2017. A commercial diesel fuel and a blend containing hydrotreated vegetable oil (HVO) 15% in vol were tested, both complying with the EN 590 standard. HVO consists of parafinic hydrocarbons and it is fully miscible with diesel fuel. Particulate matter was sampled in a partial diluted stream of bus exhaust, as prescribed by directive 1999/96/EC, and temperature before the filter was maintained below 52 °C (Costagliola et al., 2006). Sampling time was 20 min for each filter and the average filter loading about 0.5 mg. Filters were conditioned and weighed in a chamber maintained at a temperature within 22 ± 3 °C.

2.3.4. Urban ambient

Urban ambient filter samples were taken on top of the building of the University of Naples Federico II at a height of approximately 25 m from the 28th of February 2017 to the 3rd of March 2017. The university is located in the city center of Naples, close to the port, which is one of the largest and busiest ports of the Mediterranean. Sampling was conducted with the continuous and automated 'SWAM 5A Dual Channel' sampler from 'FAI Instruments' with a volume flow rate of 2.3 m³/h. Four 24-h samples each have been collected for the PM2.5 and the PM10 channel, whereby the filters were always changed at 00:00. Weather conditions reported for the airport of Naples, which is located approximately 5 km northeast of the university, show average temperatures for this time of the year

and rainfall on the 1st of March 2017.

2.4. Filter handling and pretreatment at CIO

After sampling, the filters were individually packed in pre-heated (2h at 550 °C) aluminum foil or separate polystyrene petri dishes, which were then placed in a separate sealable plastic bag. The samples were stored at a temperature of around −20 °C until further analysis. Tools used for filter handling, e.g. tweezers and punches, were first cleaned with Acetone, then with Ethanol and finally left to dry for at least 5 min. Some of the filter samples were submitted to water-extraction to remove water-soluble organic carbon. To that end, a punch of 1 cm^2 of the filter sample was left overnight in a covered glass petri dish with approximately 20 ml of Milli-Q water. Afterwards the filter samples were dried for at least 12 h in a desiccator filled with silica gel. During water-extraction a small portion of the water-insoluble aerosol particle material might be lost, because it is flushed from the filter surface. Filter samples were not treated for the removal of inorganic carbon.

3. Results and discussion

3.1. Measurement stability and reproducibility

Fig. 2 shows the typical reproducibility of $\delta^{13}C$ values for the routinely measured reference materials, which gives a good impression of the stability of this measurement method. Shown are the raw data for 'CAN', 'CAF' and 'LVal' (that are based on the $\delta^{13}C$ of the IRMS reference gas pulse) with values for different concentrations of the aqueous reference material solution as different symbols, all with a concentration of about 3 μg carbon per μl of the solution, over a period of almost a year. Overall these raw data are quite stable (standard deviation over the whole period is ≈0.4‰ for all three of them), and the drift patterns in the three materials coincide. For calibration, a two-point linear scale correction was applied based on the assigned values for 'CAN' and 'CAF'. 'LVal' serves as a quality control reference material and the calibrated values are shown as green triangles for the whole time period. Prior to calibration, outliers that differ by twice the standard deviation or more from the mean raw value have been excluded, they are not shown in Fig. 2. The excluded data are shown as yellow triangles in Fig. A.2 in the appendix. The calibrated data of 'LVal' have a standard deviation of 0.19‰, and variability is greatly reduced after calibration. The average value of $\delta^{13}C$ of 'LVal' after calibration is −24.10‰ with a standard error of 0.01‰. Although it is different from the nominal value of −24.03‰, this is not significant with respect to the uncertainty caused by the calibration of the data, and the standard error.
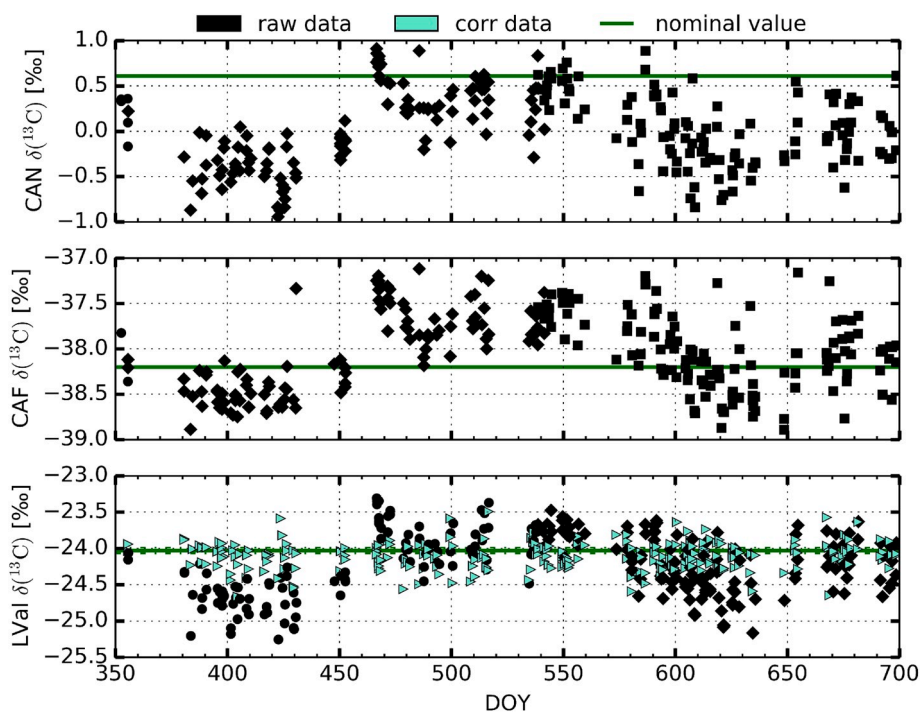

Fig. 2. Overview of reference materials: raw data (that are based on the $\delta^{13}C$ of the IRMS reference gas pulse) of 'CAN', 'CAF', 'LVal' (black) and the calibrated data of 'LVal' (green triangles) based on the calibration using the assigned values for 'CAN' and 'CAF' (green lines) shown as a function of time. Different symbols correspond to different reference material solutions, all with a concentration of about 3 μg carbon per μl of the solution. (For interpretation of the references to color in this figure legend, the reader is referred to the Web version of this article.)

Although the principles of the two point calibration are clear, there are a number of ways to perform this in practice. The shown data are the result of the best out of three different investigated methods. One set of 'CAN', 'CAF', and 'LVal' are measured both at the beginning and the end of the day. All samples are subsequently calibrated using the set of 'CAN'-'CAF' closest by in time ('default' method). Two simpler methods were investigated to check possibilities to decrease time and workload of measurements. In the 'daily average' method the average of all values measured for 'CAN' or 'CAF' within a measurement day is used to obtain the two-point calibration. All data measured on that specific day are then corrected with this relation neglecting the diurnal trend. The third method 'stable periods' averages all values of 'CAN' and 'CAF', which show a relative stability over a specific time period. These averages are used to correct all measured data in the respective time period. Corrected and raw data of all methods with the root mean square error (RMSE) with respect to the nominal value of 'LVal' are shown in Fig. A.3 in the appendix. The 'default' correction method shows the lowest RMSE and was used to process all data.

The memory effect, which describes the influence of previous samples on the actual measurement in the IRMS, was also tested. The experiments were comprised of three repeated measurements of a known reference material followed by three repeated measurement of a reference material with a significantly different $\delta^{13}C$ value. In total six experiments were conducted, two with a series of 'CAF' followed by a series of 'CAN', two with first a series of 'CAN' and then 'CAF' and two experiments where first a series of 'CAN' was measured, then a series of a reference material with a $\delta^{13}C$ value of $-14.48‰$ and then a series of 'CAF'. All six experiments showed the memory effect to be negligible.

Fig. 3 shows results for the $\delta^{13}C$ value for repeated analysis of two different aerosol filter samples. It shows a good reproducibility for all three different temperature steps over a long time period. In between the two measurement periods the IRMS tuning was changed and a new filament had to be installed. Data from the first period (DOY 174–187) were calibrated according to the 'stable periods' two-point linear relation, because reference materials were not measured on a daily basis in the beginning. Data from the second period (DOY 318–355) are calibrated with the 'default' correction method. For this reason data from the first period show a significant drift over the measurement period and are more variable than data from the second period. The standard deviation of the calibrated results over both time periods for filter 'V130801' is 0.6‰ for 200 °C, 0.5‰ for 350 °C and 0.4‰ for 650 °C. For filter 'V130830' these standard deviations are as follows: 0.26‰ for 200 °C, 0.25‰ for 350 °C and 0.24‰ for 650 °C. Standard deviations for filter 'V130830' are smaller, as there are less measurements done for this filter in the first time period. This shows very clearly the influence of the used calibration method. The averaged standard deviations of both filter for the second time period are used as an uncertainty estimate for the $\delta^{13}C$ value of filter sample measurements (0.31‰ for 200 °C, 0.28‰ for 350 °C and 0.35‰ for 650 °C).

3.2. Isotopic fractionation

Ideally a specific organic compound should be desorbed at a temperature well above its melting point to ensure that all CO_2 originating from this compound can be analyzed and fractionation is avoided, as shown for the case of L-Valine in the previous section. As an aerosol filter sample contains many different organic compounds with different melting points, this can not be guaranteed for all the compounds. For a specific set of temperature steps, it will invariably happen that a few compounds are only partially desorbed at a certain temperature step and the rest is analyzed during the following temperature step. This partial desorption will likely be accompanied by isotopic fractionation. If this fractionation has a strong influence on the $\delta^{13}C$ value measured at a specific temperature step, the measured $\delta^{13}C$ values of a filter sample would depend on method parameters as the number and the magnitude of the chosen temperature steps (Dusek et al., 2013). To investigate the possible influence of isotopic fractionation in the process with our choice of temperature steps, we measured different reference materials at those different temperature steps and compared the resulting $\delta^{13}C$ values to the nominal value.

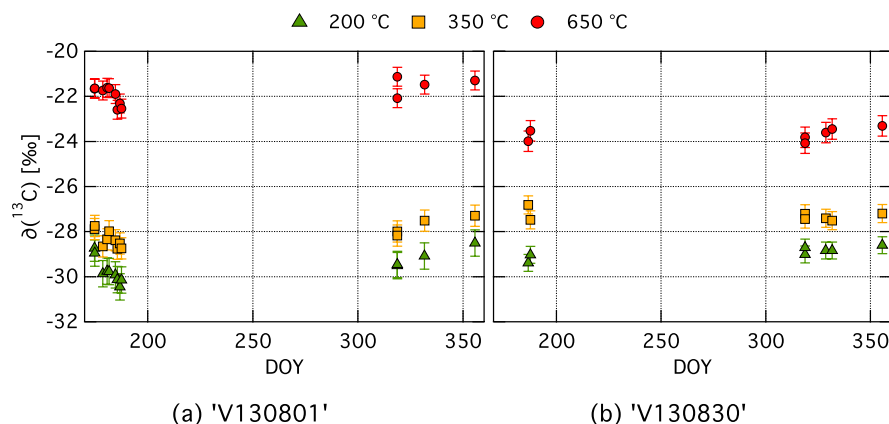**Fig. 3. Repeated analysis** of two ambient aerosol filters. $\delta^{13}C$ values for different temperature steps are shown with different colors, the standard deviation is shown as uncertainty bars. (For interpretation of the references to color in this figure legend, the reader is referred to the Web version of this article.)

Fig. 4 shows the δ^{13}C values (calibrated with the 'default' method) and the fraction of total OC mass desorbed for 'CAN' (a), 'CAF' (b), 'LVal' (c) and sucrose (d) measured at our regular three different temperature steps (200 °C, 350 °C, 650 °C). Blue and green bars/ marker correspond to different volumes of the reference material solution (5 μl and 10 μl). For the caffeine solutions ('CAN' and 'CAF') one μl corresponds to a total OC mass of 3.4 μg. For the 'LVal' solution one μl corrsponds to 3.2 μg total OC mass and for the sucrose solution one μl results in 2.8 μg total OC mass. The data are the average of two repeated analyses for each solution type and solution volume for 'CAN', 'CAF' and 'LVal'. For sucrose two analyses have been done using 5 μl and three using 10 μl, also the averaged values are shown.

Caffeine has a melting point of 235 °C (Agafonova, Moshchenskii & Tkachenko, 2012), but evaporation from the solid phase is already significant at lower temperatures. Approximately 80% of the total OC mass was desorbed already at 200 °C, 20% at 350 °C and at 650 °C OC masses lower than the detection limit of the IRMS were observed. The δ^{13}C value at 200 °C, where most of the caffeine was desorbed was very close to the nominal value and ^{13}C values at 350 °C are slightly enriched with respect to the nominal value. This observation is consistent with the process of kinetic fractionation, but the shown enrichment is not very significant and lies within the measurement reproducibility.

A δ^{13}C value for total desorbed OC can be estimated as a weighted average of the δ^{13}C values measured at the individual temperature steps. δ^{13}C of total OC for 'CAN' was approximately 0.78‰ for a volume of 5 μl and 0.89‰ for 10 μl. For 'CAF' it was −37.85‰ for 5 μl and −37.94‰ for 10 μl. The fractionation was less than 1‰ for desorption at different temperature steps and the δ^{13}C value of total desorbed OC was identical to the nominal value within uncertainty. In summary no significant isotopic fractionation was observed for the shown experiments with 'CAN' and 'CAF'. The uncertainty bars of the δ^{13}C values in Fig. 4 are averages of the standard deviations of both repeated filters shown in Fig. 3 from the second measurement period. This presents our best uncertainty estimation for desorption at different temperature steps, but is most likely an overestimate for reference materials. Both 'CAN' and 'CAF' show similar trends concerning the OC masses and the δ^{13}C values for the different temperature steps, which is obvious as both are the same chemical compound, namely caffeine. Different volumes of the reference material solution, resulting in different reference material masses applied to the filter, also show similar δ^{13}C values, except the δ^{13}C value at 350 °C for 'CAN'.

The experiments with L-Valine and sucrose solutions show, as already observed for caffeine, that the δ^{13}C value at the temperature
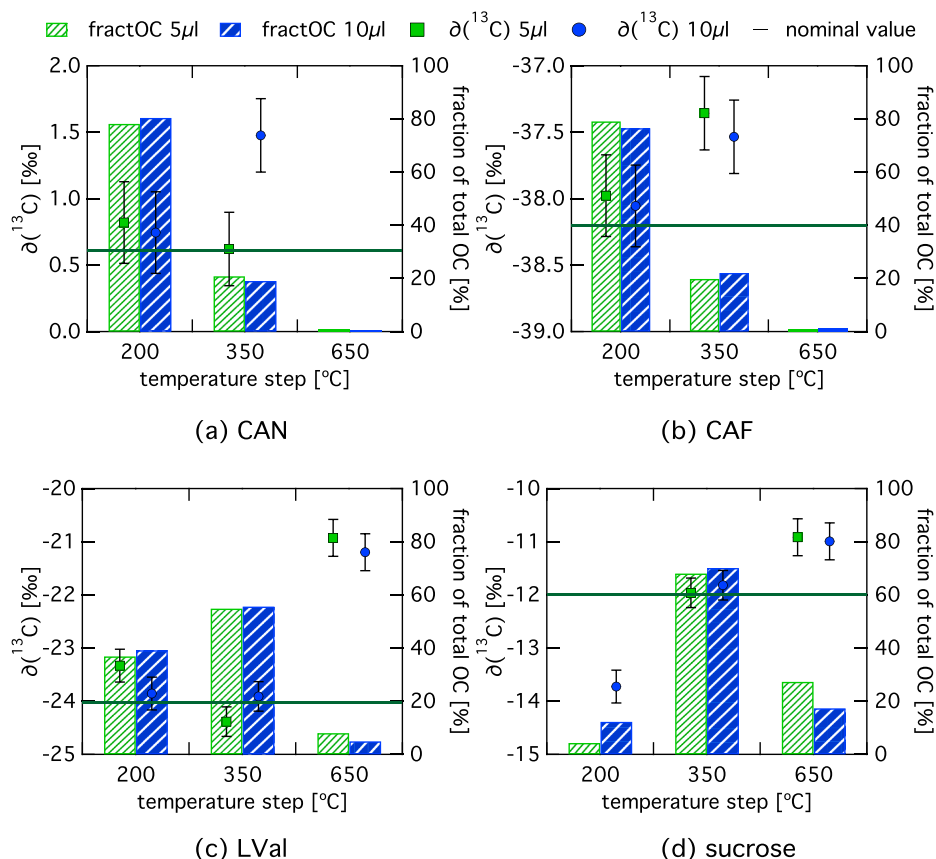

Fig. 4. **Isotopic fractionation tests**: solutions of 'CAN', 'CAF', 'LVal' and sucrose analyzed at three different temperature steps (200 °C, 350 °C, 650 °C), bars show the fraction of total OC mass desorbed at the respective temperature step and the markers show δ^{13}C values, the horizontal green lines correspond to the reference values, and different colors to different volumes of the solutions that have been analyzed. (For interpretation of the references to color in this figure legend, the reader is referred to the Web version of this article.)

where most of the OC was desorbed, in both cases 350 °C, is closest to the nominal value. L-Valine has a decomposition point of 298 °C, which lies between the first and the second temperature step. Approximately 40% of the OC mass of 'LVal' was desorbed at 200 °C and around 55% at 350 °C. δ^{13}C values for both temperature steps are similar and are close to the nominal value. In contrast at 650 °C the desorbed OC mass fraction was much lower, about 7%, and the δ^{13}C value shows a clear enrichment with respect to the nominal value. The δ^{13}C values of total OC are −23.71‰ for 5 μl and −23.75‰ for 10 μl of 'LVal' solution. Both are very similar and agree within the range given by reproducibility with the nominal value of −24.03‰. The sucrose solution (Sigma Aldrich, CAS No. 57-50-1, purity $\geq$99.5%) is not produced from known δ^{13}C reference material, but it is normally used in calibration of the OC-EC analyzer. Its δ^{13}C value was measured three times at a desorption temperature of 650 °C and the average with standard deviation of −11.99 ± 0.14‰ is shown as nominal value. Sucrose is also a very good example for the process of kinetic isotopic fractionation. Between about 4% and 12% of the total OC mass, depending on the analyzed volume, were desorbed at 200 °C, resulting in a depleted δ^{13}C value with respect to the nominal value. Most OC mass (about 70%) was desorbed at 350 °C and the respective δ^{13}C value is very close to the nominal value. At 650 °C 27% of OC was desorbed for 5 μl of the solution and 17% for 10 μl causing the δ^{13}C values to be enriched compared to the nominal value. The δ^{13}C values for total OC of sucrose are −11.66‰ for 5 μl and −11.91‰ for 10 μl. Both for 'LVal' and sucrose the partial desorption and the resulting isotopic fractionation for the separate temperature steps do not have an influence on the combined δ^{13}C value, which agrees with the nominal value within the range of uncertainty. This observation is especially important for sucrose, as sucrose is also known to char at lower temperatures in helium. Charring is the process of partial transformation of OC to EC-like material, which then can only be removed by combustion and is lost for δ^{13}C analysis of OC. Both charring and partial isotopic fractionation can be excluded as affecting processes for this measurement method.

Ambient aerosol filter samples have been analyzed both with three temperature steps (200 °C, 350 °C, 650 °C) and with only one step at 650 °C. The latter produces a good approximation of the δ^{13}C of total OC. Similar to the experiments with reference materials described above, δ^{13}C of OC can also be estimated from a weighted average of δ^{13}C values, measured at individual temperature steps. Fig. 5 shows the calculated δ^{13}C values of OC versus the δ^{13}C of OC measured directly at 650 °C. Furthermore in Fig. 5 the sum of OC masses from the three different temperature steps is shown versus the OC mass of compounds desorbed only during one step at 650 °C. The linear fit of the δ^{13}C values shows a slope of approximately 1, which means the results for δ^{13}C of total OC are not dependent on the number of used temperature steps. Desorption at three different temperature steps and especially at lower temperatures causes different charring and isotopic fractionation than at only one step at high temperature, where ideally no fractionation occurs since all OC is desorbed. If charring and isotopic fractionation would have a significant influence on the resulting δ^{13}C values, the results calculated from three temperature steps would differ more from the observed δ^{13}C values at 650 °C. The δ^{13}C values at individual temperature steps are influenced to some extent by isotopic fractionation (example of sucrose, Fig. 4). However, in real aerosol samples
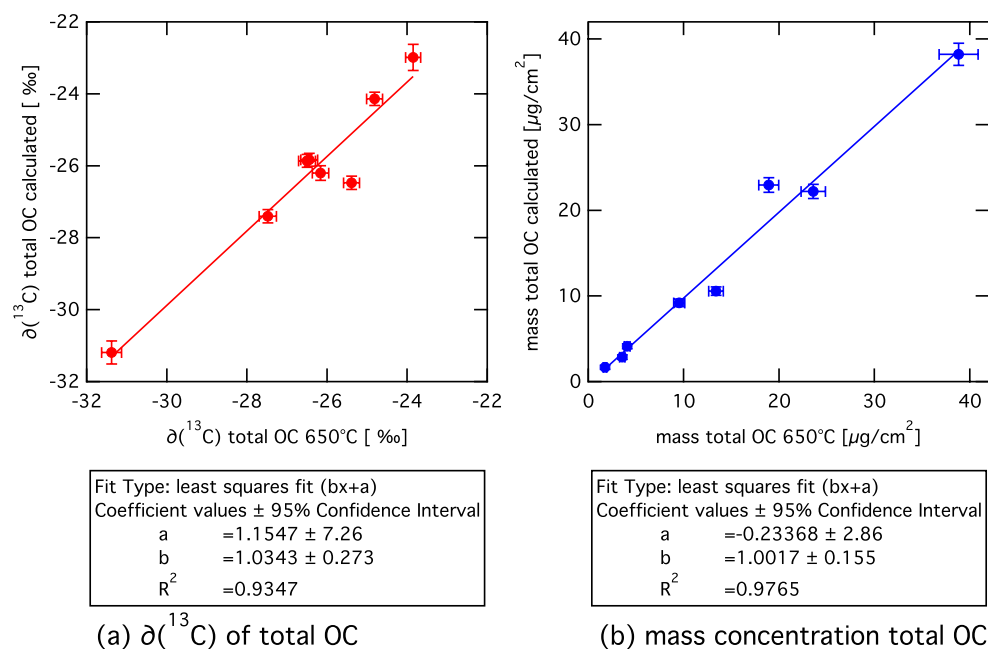

| Fit Type: least squares fit (bx+a) |
| Coefficient values ± 95% Confidence Interval |
| a   =1.1547 ± 7.26 |
| b   =1.0343 ± 0.273 |
| R^2 =0.9347 |

| Fit Type: least squares fit (bx+a) |
| Coefficient values ± 95% Confidence Interval |
| a   =-0.23368 ± 2.86 |
| b   =1.0017 ± 0.155 |
| R^2 =0.9765 |

(a) $\delta(^{13}C)$ of total OC

(b) mass concentration total OC

Fig. 5. Isotopic fractionation tests: (a) shows calculated δ^{13}C values (weighted average of ^{13}C values, measured at individual temperature steps) of OC versus the δ^{13}C of OC measured directly at 650 °C; error bars for calculated δ^{13}C values are estimated from the repeated filter analysis (see Fig. 3) and for δ^{13}C measured directly at 650 °C estimated from repeated calibrated 'LVal' data (standard deviation of 0.19‰) (b) shows the sum of analyzed OC mass concentration from the individual temperatures steps versus the OC mass concentration measured directly at 650 °C; uncertainty estimation is done by the OC-EC analyzer software.

a small fraction of enriched compounds remaining from the previous temperature step is always mixed up with other compounds that are also desorbed at the same temperature step. Since the δ^{13}C value only differs strongly from the nominal value, if a small fraction of the original material is left over, this influence should be relatively small. The comparison of the OC mass only from 650 °C and the sum from all the different temperature steps also leads to the conclusion, that there is no strong difference between charring at the different temperatures to charring at only 650 °C. If charring would be stronger for lower temperatures the charred carbon material would not be analyzed with the described methods, as it can not be released from the filter in helium.

3.3. δ^{13}C signatures of various emission sources

Fig. 6 and Table 1 show the results from the δ^{13}C source study. The δ^{13}C of OC for the different sources desorbed at the three different temperatures (200 °C, 350 °C, 650 °C) represent averaged values of all analyzed samples (3–6) from the respective source and the uncertainty bars show the standard deviation of these measurements. Measurement results for all individual filter samples are shown in a dataset published along with this manuscript. In addition to the δ^{13}C values shown in Fig. 6, Table 1 also gives δ^{13}C of total OC, calculated by a weighted average of δ^{13}C measured at the individual temperature steps. Fig. 6 also shows the averaged OC to EC ratios for each source and the respective standard deviation. For 'Quercus ilex' OC/EC ratios were calculated as OC concentrations measured on untreated filters divided by EC concentrations on water-extracted filters.

We investigated two different typical ways of biomass burning in the Naples region. One is the combustion of wood pellets and the other the combustion of twigs, in our case twigs from a common type of Mediterranean oak, the 'Quercus ilex'. 'Quercus ilex' samples show the highest OC to EC ratio of more than 11 on average. In contrast, particles from pellet combustion show an OC to EC ratio of only about 1. Pellet burners work at higher temperatures and have more efficient combustion, which results in much less OC and more EC (and overall less TC). The standard deviation for the 'Quercus ilex' samples is much higher than for the combustion of pellets, which is mainly caused by the high sensitivity of the OC to EC ratio to combustion conditions. Combustion of homogeneously produced pellets is most likely more reproducible than the combustion of very variable random twig material (thickness and size variation) from the Quercus ilex tree. Samples of bus exhaust aerosol show the lowest OC/EC ratio of approximately 0.26. Only a marginal difference was found between the new type of fuel, which contains hydrotreated vegetable oil, and the commercial diesel (see dataset published with this article). The respective values are 0.25 ± 0.06 (average and standard deviation of 3 samples) and 0.28 ± 0.02. OC/EC ratios of urban background aerosols collected at the roof of the university in the different size ranges PM2.5 and PM10 are very similar and both show a high standard deviation. OC/EC ratios of ambient aerosol are usually more variable depending mostly on meteorological parameters and nearby sources. The OC/EC ratios of the tunnel samples lie in between the observed values for bus exhaust and ambient aerosol and show a lower standard deviation than the ambient filter samples. The tunnel air of course contains nearly exclusively aerosol particles from vehicle exhaust emissions, but it has higher OC/EC ratios than the directly measured bus exhaust, due to a realistic mix of newer and older cars and real world driving conditions.

δ^{13}C values of total OC shown in Table 1 vary in a narrow range of about $-28‰$ to $-26‰$ (value of tunnel filter not included), which makes a clear distinction between different sources difficult. However, δ^{13}C measured at different temperatures provide information that potentially allow more detailed conclusions about source contributions. An example for this is the bus exhaust sample
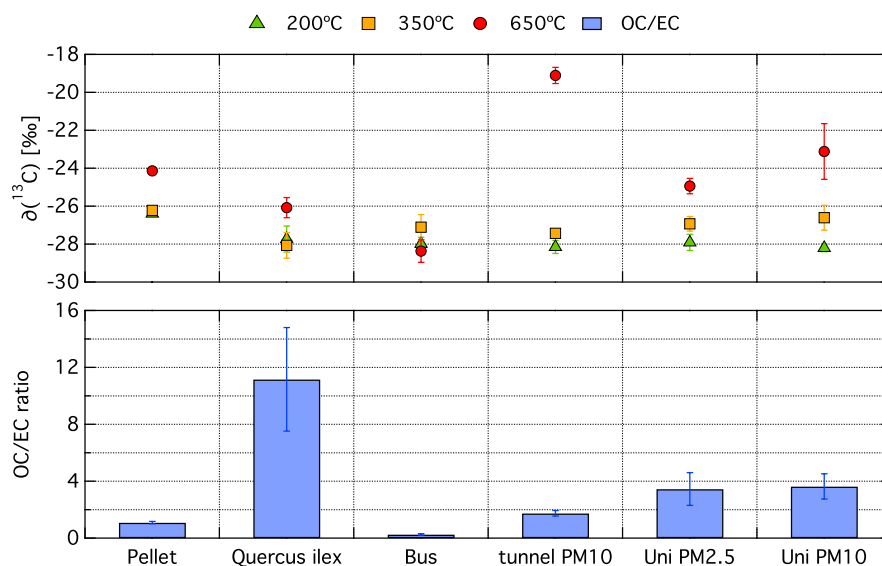

Fig. 6. **Source study**: δ^{13}C values of OC desorbed at different temperatures and OC/EC ratios for different investigated sources, shown are averaged values of all analyzed samples. The error bars correspond to the standard deviation of the different samples.

Table 1

Overview of results: OC/EC ratios and δ^{13}C signatures of various emission sources and ambient filter from the Naples region; shown are averaged values and their standard deviations with the sample size.

sample type	pellets	Quercus ilex	bus exhaust	tunnel PM10	Uni PM2.5	Uni PM10
sample size	3	3	4	6	4	4
OC/EC AV	1.08	11.12	0.26	1.73	3.39	3.59
OC/EC σ	0.08	3.62	0.05	0.19	1.10	0.85
$\delta^{13}C_{OC}$ 200 °C AV [‰]	−26.39	−27.72	−27.98	−28.15	−27.91	−28.20
$\delta^{13}C_{OC}$ 200 °C σ [‰]	0.15	0.69	0.34	0.34	0.43	0.20
$\delta^{13}C_{OC}$ 350 °C AV [‰]	−26.22	−28.07	−27.10	−27.42	−26.93	−26.60
$\delta^{13}C_{OC}$ 350 °C σ[‰]	0.09	0.68	0.67	0.21	0.38	0.66
$\delta^{13}C_{OC}$ 650 °C AV [‰]	−24.14	−26.07	−28.37	−19.11	−24.94	−23.12
$\delta^{13}C_{OC}$ 650 °C σ [‰]	0.15	0.53	0.60	0.42	0.41	1.47
$\delta^{13}C_{OC}$ total AV [‰]	−25.83	−27.57	−27.83	–	−26.64	−25.78
$\delta^{13}C_{OC}$ total σ [‰]	0.12	0.68	0.07	–	0.36	0.66

and the 'Quercus ilex' sample. They show almost the same δ^{13}C value for total OC, but for 'Quercus ilex' the δ^{13}C is depleted at 350 °C and at 650 °C it is enriched compared to the bus exhaust. Nonetheless a quantitative source apportionment based on δ^{13}C is not possible for the major sources in the Naples region, since the δ^{13}C values are not distinctive enough. This was also observed in (Martinsson et al., 2017). Source apportionment relying mainly on δ^{13}C values of aerosol samples is only successful for regions where the main sources are clearly distinguishable on the basis of stable carbon analysis, like shown in (Masalaite et al., 2017) for Lithuania. In other regions, it is always advisable to use a more distinctive tracer like ^{14}C, which allows the clear differentiation of fossil and contemporary sources, or specific source apportionment tracers like levoglucosan. This makes the analysis more time and labor intense, but allows a more reliable and significant source apportionment.

For some samples an enrichment in ^{13}C at the 650 °C temperature step compared to the other temperatures was observed. This difference was very large for the tunnel filter samples, but also strongly present in the ambient samples from the university, where PM10 filter samples showed a stronger enrichment than the PM2.5 samples at 650 °C. Presumably this is caused by the presence of carbonate carbon in these samples, which was not removed by acidification. One source of carbonate carbon is road dust, which explains the strongest influence in the tunnel filter. Furthermore another indicator for this source is the stronger influence on PM10 filter, as road dust is strongly present in the coarse mode, whereas road dust is not present in the direct bus exhaust measurements. Pre-treatment to remove carbonate carbon before δ^{13}C analysis is advisable, but more testing for this study was unfortunately not possible due to a lack of filter sample material. One should keep in mind that for the results shown in this study carbon desorbed at the 650 °C temperature step is likely a mixture of organic and carbonate carbon, at least for PM10. Experiments with acid pre-treatment to remove the carbonate carbon were conducted in a very recent study by (Masalaite et al., 2020). They found that acidification of the filter samples with HCl fumes before δ^{13}C analysis caused obvious artifacts of the desorbed OC mass and the δ^{13}C value at a temperature of 650 °C. They instead recommend analyzing the samples at 550 °C as the highest desorption temperature step to obtain trustworthy δ^{13}C results, because CaCO$_3$ does only desorb at temperatures above 550 °C. Nevertheless for the future more tests regarding the removal of carbonate carbon from doubtful filter samples are advisable.

Comparing δ^{13}C for the sources typical for the Naples region to values for similar sources from previous studies shows good agreement. TC of aerosol particles produced during controlled biomass burning (Garbaras et al., 2015) showed a δ^{13}C value of −26.9 ± 0.2‰ for wood pellets of unknown origin, which is slightly more depleted than the measured value of −25.8 ± 0.1‰ for total OC in this study. Experiments where particles are collected that originate from combustion in a controlled chamber environment are rare. More often the practice is to compare δ^{13}C values of aerosol particles to values determined directly from possible source materials like biomass or fuel samples. For biomass burning chamber experiments (Garbaras et al., 2015) observed a difference between the collected aerosol particle and the original source of −0.94‰ to 1.12‰. Other studies [(Martinsson et al., 2017), and references therein] found δ^{13}C values of biomass material of trees from the genus 'Quercus' in a range of −26.4‰ to −29.4‰. The most comparable material to our study were branches and they showed a δ^{13}C value of −28.8 ± 0.8‰. The difference to the total OC δ^{13}C of −27.6 ± 0.7‰ from the 'Quercus ilex' could be caused by isotopic fractionation during the combustion of the material or by the different growing conditions of this wood type. Both types of biomass burning samples show an enrichment for values measured at 650 °C compared to the other temperature steps. This enrichment is most likely caused by cellulose combustion products desorbing at higher temperatures compared to combustion products of the more volatile lipids that are known to be depleted in ^{13}C compared to carbohydrates as described in (Czimczik, Preston, Schmidt, Werner, & Schulze, 2002). Several studies (Widory, 2006; Martinsson et al., 2017; Mašalaitė, Garbaras, & Remeikis, 2012; Aguilera & Whigham, 2018; Masalaite et al., 2017) investigated the stable carbon isotopes in diesel fuel and found a value of δ^{13}C varying widely, between −24.2‰ to −31.6‰ depending on the source region of the crude oil. Isotopic fractionation during the production of aerosol particles from fossil fuel combustion was determined to be around −1.9‰ for diesel (Widory, 2006). δ^{13}C values for the bus exhaust samples in our study are in the range of −27.1‰ to −28.4‰ for the different temperatures and −27.8 ± 0.1‰ for total OC. This corresponds with western diesel fuel types as found in (Mašalaitė, Garbaras, & Remeikis, 2012). Neglecting the δ^{13}C value at 650 °C due to possible influence of carbonate carbon, δ^{13}C of the tunnel samples is very similar to the bus exhaust

samples. Measurements of $\delta^{13}C$ in OC of filter samples from urban areas (China, Canada) with strong influence from vehicle emissions found very similar results to our urban filter samples in a range of $-26.3‰$ to $-28.1‰$ (Aguilera & Whigham, 2018).

4. Conclusions

It was shown that our methodology to analyze ^{13}C in organic carbon from aerosol filter samples delivers $\delta^{13}C$ with a sufficient accuracy and precision. Furthermore, we conclude that the presented method is not dependent on the number of used temperature steps and charring or isotopic fractionation during thermal desorption is not affecting the resulting $\delta^{13}C$ values for OC.

The thermal desorption method was applied to filter samples of various emission sources and ambient filters from the region of Naples to determine the $\delta^{13}C$ signatures in OC. Thereby it was found that for ambient and the tunnel filter samples there is evidence that carbonate carbon causes an enrichment in ^{13}C at the 650 °C temperature step, which should be further investigated.

$\delta^{13}C$ signatures of the major OC sources within the Naples area were all lying within a narrow range ($-28‰$ to $-26‰$), that was also close to $\delta^{13}C$ values of the ambient filters. Therefore it was for this region in Italy not possible to do a source apportionment only based on the $\delta^{13}C$ signatures. Since the $\delta^{13}C$ values of the ambient samples vary within the range of primary sources, this is an indication that oxidative processing and secondary organic aerosol formation do not significantly alter ^{13}C signatures in this urban location during winter time.
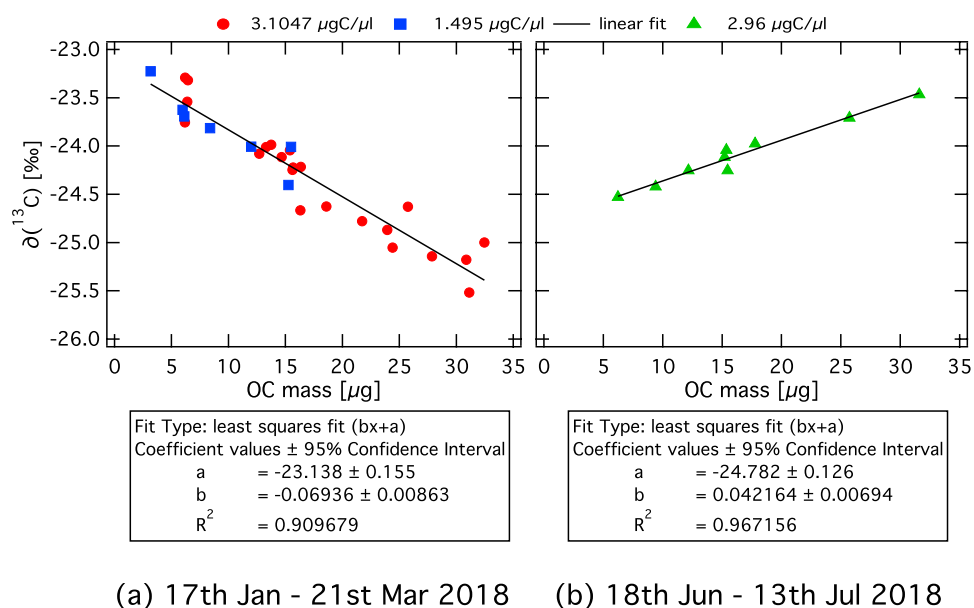
Acknowledgement

Appendix

Fig. A.1. Linearity tests with 'LVal' reference material showing a clear mass dependency of $\delta^{13}C$. All results measured in the respective time period (a) and (b) have been corrected according to the relation given by the shown linear fit.

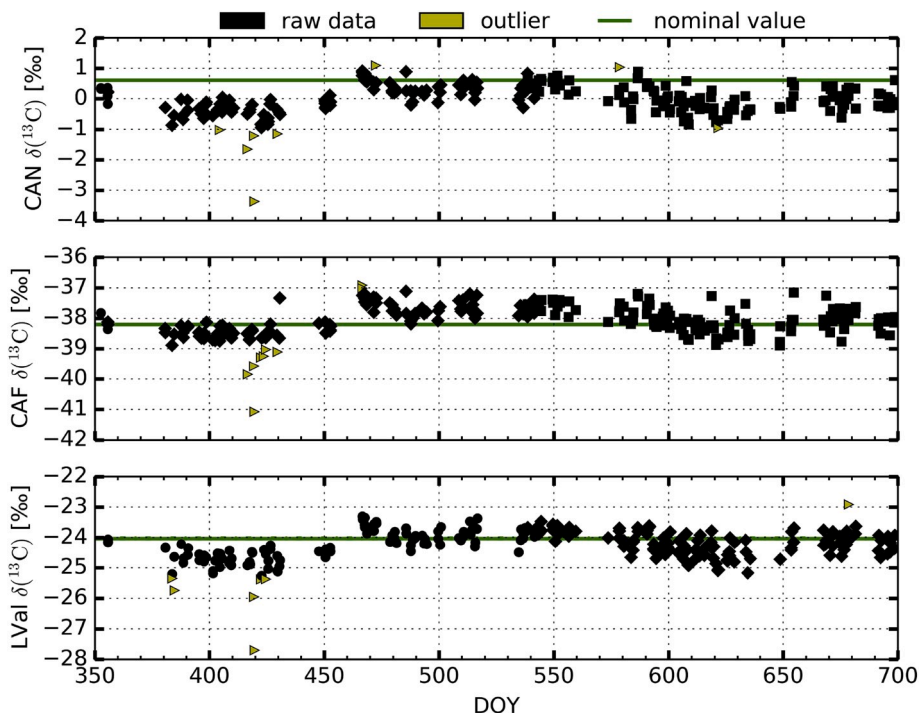**Fig. A.2. Reference material outlier**: raw data (that are based on the δ^{13}C value of the IRMS reference gas pulse) of 'CAN', 'CAF' and 'LVal' (black) shown as a function of time, green lines show the nominal δ^{13}C values. Different symbols correspond to different used reference material solutions, all with a concentration of about 3 µg carbon per µl of the solution. Yellow triangles show outlier (deviate twice the standard deviation or more from the mean value of the raw data), which are not included in calculations for the calibration of the data.
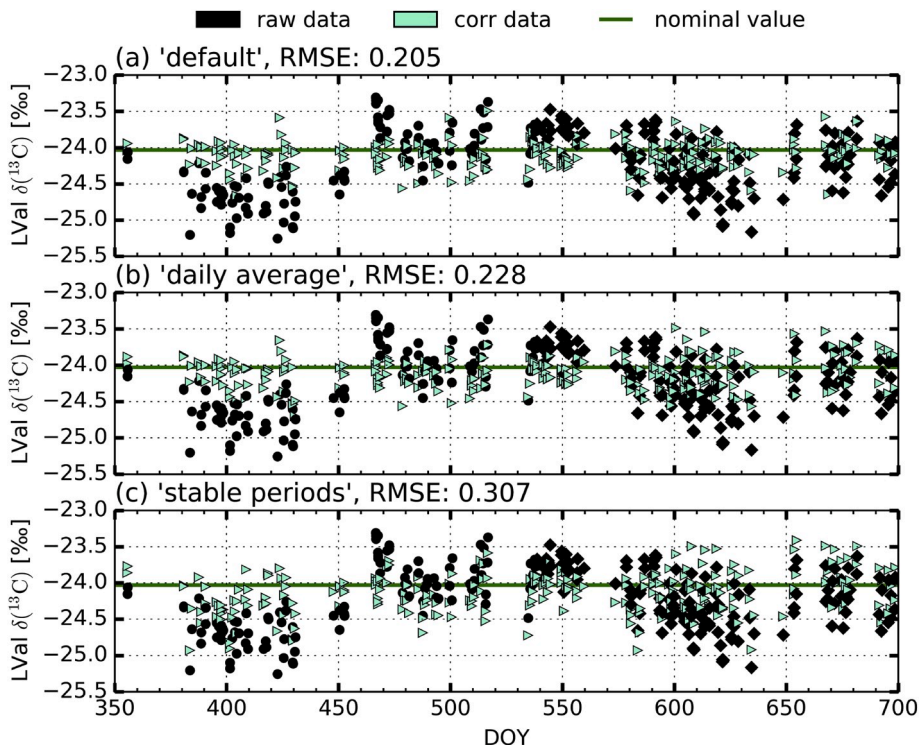

Fig. A.3. Comparison of two-point linear scale calibration methods: raw data (that are based on the δ^{13}C value of the IRMS reference gas pulse) of 'LVal' (black) and the calibrated data of 'LVal' (green triangles) based on the calibration using the assigned values for 'CAN' and 'CAF' shown as a function of time. Different symbols correspond to different used reference material solutions, all with a concentration of about 3 µg carbon per µl of

the solution. Green lines show the nominal $\delta^{13}C$ value of 'LVal'. The RMSE for each method is given in the respective header, the RMSE of the raw data of 'LVal' is 0.477.

References

Agafonova, E. V., Moshchenskii, Y. V., & Tkachenko, M. L. (2012). Determining the main thermodynamic parameters of caffeine melting by means of DSC. *Russian Journal of Physical Chemistry, 86*(6), 1147–1149. https://doi.org/10.1134/S0036024412060027.

Agnihotri, R., Mandal, T. K., Karapurkar, S. G., Naja, M., Gadi, R., Ahammmed, Y. N., et al. (2011). Stable carbon and nitrogen isotopic composition of bulk aerosols over India and northern Indian Ocean. *Atmospheric Environment, 45*(17), 2828–2835. https://doi.org/10.1016/j.atmosenv.2011.03.003. http://www.sciencedirect.com/science/article/pii/S135223101100238X.

Aguilera, J., & Whigham, L. D. (2018). Using the $^{13}C/^{12}C$ carbon isotope ratio to characterise the emission sources of airborne particulate matter: A review of literature. *Isotopes in Environmental and Health Studies, 54*(6), 573–587. https://doi.org/10.1080/10256016.2018.1531854.

Allison, C. E., Francey, R. J., & Meijer, H. A. J. (1995). *Recommendations for the reporting of stable isotope measurements of carbon and oxygen in CO$_2$ gas*. Tech. Rep. IAEA-TECDOC–825.

Boucher, O., Randall, D., Artaxo, P., Bretherton, C., Feingold, G., Forster, P., et al. (2013). Clouds and aerosols. In T. Stocker, D. Qin, G.-K. Plattner, M. Tignor, S. Allen, J. Boschung, et al. (Eds.), *Climate change 2013: The physical science basis. Contribution of working group I to the fifth assessment report of the intergovernmental panel on climate change* (pp. 571–658). Cambridge, United Kingdom and New York, NY, USA: Cambridge University Press. book section 7.

Cachier, H., Buat-Ménard, P., Fontugne, M., & Chesselet, R. (1986). Long-range transport of continentally-derived particulate carbon in the marine atmosphere: Evidence from stable carbon isotope studies. *Tellus B: Chemical and Physical Meteorology, 38B*(34), 161–177. https://doi.org/10.1111/j.1600-0889.1986.tb00184.x.

Cao, J.-J., Chow, J. C., Tao, J., Lee, S.-C., Watson, J. G., Ho, K.-F., et al. (2011). Stable carbon isotopes in aerosols from Chinese cities: Influence of fossil fuels. *Atmospheric Environment, 45*(6), 1359–1363. https://doi.org/10.1016/j.atmosenv.2010.10.056. http://www.sciencedirect.com/science/article/pii/S135223101001037X.

Cavalli, F., Viana, M., Yttri, K. E., Genberg, J., & Putaud, J. P. (2010). Toward a standardised thermal-optical protocol for measuring atmospheric organic and elemental carbon: The EUSAAR protocol. *Atmospheric Measurement Techniques, 3*(1), 79–89. https://doi.org/10.5194/amt-3-79-2010. http://www.atmos-meas-tech.net/3/79/2010/.

Ceburnis, D., Garbaras, A., Szidat, S., Rinaldi, M., Fahrni, S., Perron, N., et al. (2011). Quantification of the carbonaceous matter origin in submicron marine aerosol by ^{13}C and ^{14}C isotope analysis. *Atmospheric Chemistry and Physics, 11*(16), 8593–8606. https://doi.org/10.5194/acp-11-8593-2011. http://www.atmos-chem-phys.net/11/8593/2011/.

Chesselet, R., Fontugne, M., Buat-Ménard, P., Ezat, U., & Lambert, C. E. (1981). The origin of particulate organic carbon in the marine atmosphere as indicated by its stable carbon isotopic composition. *Geophysical Research Letters, 8*(4), 345–348. https://doi.org/10.1029/GL008i004p00345. https://agupubs.onlinelibrary.wiley.com/doi/pdf/10.1029/GL008i004p00345. https://agupubs.onlinelibrary.wiley.com/doi/abs/10.1029/GL008i004p00345.

Costagliola, M. A., Del Giacomo, N., Iaccio, I., Prati, M. V., Unich, A., Violetti, I., et al. (2006). An experience with a DPF retrofitted at the exhaust of an Euro II urban bus engine. In *Proceedings of the 29th meeting on combustion* (Vol. 3, pp. 1–6).

Craig, H. (1957). Isotopic standards for carbon and oxygen and correction factors for mass-spectrometric analysis of carbon dioxide. *Geochimica et Cosmochimica Acta, 12*(1), 133–149. https://doi.org/10.1016/0016-7037(57)90024-8. http://www.sciencedirect.com/science/article/pii/0016703757900248.

Czimczik, C. I., Preston, C. M., Schmidt, M. W. I., Werner, R. A., & Schulze, E.-D. (2002). Effects of charring on mass, organic carbon, and stable carbon isotope composition of wood. *Organic Geochemistry, 33*(11), 1207–1223. https://doi.org/10.1016/S0146-6380(02)00137-7. http://www.sciencedirect.com/science/article/pii/S0146638002001377.

Donahue, N. M., Robinson, A. L., & Pandis, S. N. (2009). Atmospheric organic particulate matter: From smoke to secondary organic aerosol. *Atmospheric Environment, 43*(1), 94–106. https://doi.org/10.1016/j.atmosenv.2008.09.055. http://www.sciencedirect.com/science/article/pii/S1352231008009229.

Dusek, U., Meusinger, C., Oyama, B., Ramon, W., de Wilde, P. A., Holzinger, R., et al. (2013). A thermal desorption system for measuring $\delta^{13}C$ ratios on organic aerosol. *Journal of Aerosol Science, 66*, 72–82. https://doi.org/10.1016/j.jaerosci.2013.08.005. http://www.sciencedirect.com/science/article/pii/S0021850213001766.

Garbaras, A., Masalaite, A., Garbariene, I., Ceburnis, D., Krugly, E., Remeikis, V., et al. (2015). Stable carbon fractionation in size-segregated aerosol particles produced by controlled biomass burning. *Journal of Aerosol Science, 79*, 86–96. https://doi.org/10.1016/j.jaerosci.2014.10.005. http://www.sciencedirect.com/science/article/pii/S0021850214001712.

Gensch, I., Kiendler-Scharr, A., & Rudolph, J. (2014). Isotope ratio studies of atmospheric organic compounds: Principles, methods, applications and potential. *International Journal of Mass Spectrometry, 365 – 366*, 206–221. https://doi.org/10.1016/j.ijms.2014.02.004, 0 http://www.sciencedirect.com/science/article/pii/S1387380614000591.

Ho, K. F., Lee, S. C., Cao, J. J., Li, Y. S., Chow, J. C., Watson, J. G., et al. (2006). Variability of organic and elemental carbon, water soluble organic carbon, and isotopes in Hong Kong. *Atmospheric Chemistry and Physics, 6*(12), 4569–4576.

Huang, L., Brook, J. R., Zhang, W., Li, S. M., Graham, L., Ernst, D., et al. (2006). Stable isotope measurements of carbon fractions (OC/EC) in airborne particulate: A new dimension for source characterization and apportionment. *Atmospheric Environment, 40*(15), 2690–2705. https://doi.org/10.1016/j.atmosenv.2005.11.062. http://www.sciencedirect.com/science/article/pii/S1352231006000227.

Kirillova, E. N., Andersson, A., Sheesley, R. J., Kruså, M., Praveen, P. S., Budhavant, K., et al. (2013). ^{13}C- and ^{14}C-based study of sources and atmospheric processing of water-soluble organic carbon (WSOC) in South Asian aerosols. *Journal of Geophysical Research: Atmosphere, 118*(2), 614–626. https://doi.org/10.1002/jgrd.50130.

Lusini, I., Pallozzi, E., Corona, P., Ciccioli, P., & Calfapietra, C. (2014). Novel application of a combustion chamber for experimental assessment of biomass burning emission. *Atmospheric Environment, 94*, 117–125. https://doi.org/10.1016/j.atmosenv.2014.05.016. http://www.sciencedirect.com/science/article/pii/S135223101400363X.

Martinelli, L. A., Camargo, P. B., Lara, L. B. L. S., Victoria, R. L., & Artaxo, P. (2002). Stable carbon and nitrogen isotopic composition of bulk aerosol particles in a C4 plant landscape of southeast Brazil. *Atmospheric Environment, 36*(14), 2427–2432. https://doi.org/10.1016/S1352-2310(01)00454-X. http://www.sciencedirect.com/science/article/pii/S135223100100454X.

Martinsson, J., Andersson, A., Sporre, M. K., Friberg, J., Kristensson, A., Swietlicki, E., et al. (2017). Evaluation of ^{13}C insert in carbonaceous aerosol source apportionment at a rural measurement site. *Aerosol and Air Quality Research, 17*, 2081–2094. https://doi.org/10.4209/aaqr.2016.09.0392.

Mašalaitė, A., Garbaras, A., & Remeikis, V. (2012). Stable isotopes in environmental investigations. *Lithuanian Journal of Physics, 52*(3), 261–268.

Masalaite, A., Holzinger, R., Remeikis, V., Röckmann, T., & Dusek, U. (2017). Characteristics, sources and evolution of fine aerosol (PM1) at urban, coastal and forest background sites in Lithuania. *Atmospheric Environment, 148*, 62–76. https://doi.org/10.1016/j.atmosenv.2016.10.038. http://www.sciencedirect.com/science/article/pii/S1352231016308457.

Masalaite, A., Remeikis, V., Garbaras, A., Dudoitis, V., Ulevicius, V., & Ceburnis, D. (2015). Elucidating carbonaceous aerosol sources by the stable carbon $\delta^{13}C_{TC}$ ratio in size-segregated particles. *Atmospheric Research, 158–159*, 1–12. https://doi.org/10.1016/j.atmosres.2015.01.014. http://www.sciencedirect.com/science/article/pii/S0169809515000319.

Masalaite, A., Remeikis, V., Zenker, K., Westra, I., Meijer, H. A. J., & Dusek, U. (2020). Seasonal changes of sources and volatility of carbonaceous aerosol at urban, coastal and forest sites in Eastern Europe (Lithuania). *Atmospheric Environment*. In press.

Myhre, G., Shindell, D., Bréon, F.-M., Collins, W., Fuglestvedt, J., Huang, J., et al. (2013). Anthropogenic and natural radiative forcing. In T. Stocker, D. Qin, G.-K. Plattner, M. Tignor, S. Allen, J. Boschung, et al. (Eds.), *Climate change 2013: The physical science basis. Contribution of working group I to the fifth assessment report of the intergovernmental panel on climate change* (pp. 659–740). Cambridge, United Kingdom and New York, NY, USA: Cambridge University Press. book section 8.

Narukawa, M., Kawamura, K., Li, S.-M., & Bottenheim, J. W. (2008). Stable carbon isotopic ratios and ionic composition of the high-arctic aerosols: An increase in δ^{13}C values from winter to spring. *Journal of Geophysical Research: Atmosphere, 113*(D2).

Nel, A. (2005). Air pollution-related illness: Effects of particles. *Science, 308*(5723), 804–806. https://doi.org/10.1126/science.1108752. http://science.sciencemag.org/content/308/5723/804.full.pdf. http://science.sciencemag.org/content/308/5723/804.

Ni, H., Huang, R.-J., Cao, J., Dai, W., Zhou, J., Deng, H., et al. (2019). High contributions of fossil sources to more volatile organic carbon. *Atmospheric Chemistry and Physics Discussions*, 1–34. https://doi.org/10.5194/acp-2018-1343. https://www.atmos-chem-phys-discuss.net/acp-2018-1343/.

Ni, H., Huang, R.-J., Cao, J., Liu, W., Zhang, T., Wang, M., et al. (2018). Source apportionment of carbonaceous aerosols in Xi'an, China: Insights from a full year of measurements of radiocarbon and the stable isotope ^{13}C. *Atmospheric Chemistry and Physics, 18*(22), 16363–16383. https://doi.org/10.5194/acp-18-16363-2018. https://www.atmos-chem-phys.net/18/16363/2018/.

O'Leary, M. H. (1988). Carbon Isotopes in Photosynthesis: Fractionation techniques may reveal new aspects of carbon dynamics in plants. *BioScience, 38*(5), 328–336. https://doi.org/10.2307/1310735.

Piazzalunga, A., Bernardoni, V., Fermo, P., Valli, G., & Vecchi, R. (2011). Technical Note: On the effect of water-soluble compounds removal on EC quantification by TOT analysis in urban aerosol samples. *Atmospheric Chemistry and Physics, 11*(19), 10193–10203. https://doi.org/10.5194/acp-11-10193-2011. https://www.atmos-chem-phys.net/11/10193/2011/.

Pope III, C. A., & Dockery, D. W. (2006). Health effects of fine particulate air pollution: Lines that connect. *Journal of the Air & Waste Management Association, 56*(6), 709–742. https://doi.org/10.1080/10473289.2006.10464485.

Pöschl, U. (2005). Atmospheric aerosols: Composition, transformation, climate and health effects. *Angewandte Chemie International Edition, 44*(46), 7520–7540. https://doi.org/10.1002/anie.200501122.

Riccio, A., Chianese, E., Monaco, D., Costagliola, M. A., Perretta, G., Prati, M. V., et al. (2016). Real-world automotive particulate matter and PAH emission factors and profile concentrations: Results from an urban tunnel experiment in Naples, Italy. *Atmospheric Environment, 141*, 379–387. https://doi.org/10.1016/j.atmosenv.2016.06.070.

Riccio, A., Chianese, E., Tirimberio, G., & Prati, M. V. (2017). Emission factors of inorganic ions from road traffic: A case study from the city of Naples (Italy). *Transportation Research Part D: Transport and Environment, 54*, 239–249. https://doi.org/10.1016/j.trd.2017.05.008.

Schimmelmann, A., Qi, H., Coplen, T. B., Brand, W. A., Fong, J., Meier-Augenstein, W., et al. (2016). Organic reference materials for hydrogen, carbon, and nitrogen stable isotope-ratio measurements: Caffeines, n-alkanes, fatty acid methyl esters, glycines, L-valines, polyethylenes, and oils. *Analytical Chemistry, 88*(8), 4294–4302. https://doi.org/10.1021/acs.analchem.5b04392.

Subramanian, R., Khlystov, A. Y., & Robinson, A. L. (2006). Effect of peak inert-mode temperature on elemental carbon measured using thermal-optical analysis. *Aerosol Science and Technology, 40*(10), 763–780. https://doi.org/10.1080/02786820600714403.

Widory, D. (2006). Combustibles, fuels and their combustion products: A view through carbon isotopes. *Combustion Theory and Modelling, 10*(5), 831–841. https://doi.org/10.1080/13647830600720264.

Widory, D., Roy, S., Moullec, Y. L., Goupil, G., Cocherie, A., & Guerrot, C. (2004). The origin of atmospheric particles in Paris: A view through carbon and lead isotopes. *Atmospheric Environment, 38*(7), 953–961. https://doi.org/10.1016/j.atmosenv.2003.11.001. http://www.sciencedirect.com/science/article/pii/S1352231003010008.

Zenker, K., Vonwiller, M., Szidat, S., Calzolai, G., Giannoni, M., Bernardoni, V., et al. (2017). Evaluation and inter-comparison of oxygen-based OC-EC separation methods for radiocarbon analysis of ambient aerosol particle samples. *Atmosphere, 8*. https://doi.org/10.3390/atmos8110226. http://www.mdpi.com/2073-4433/8/11/226.